Progress In Electromagnetics Research, Vol. 142, 625–638, 2013

BROADBAND MILLIMETERWAVE METAMATERIAL ABSORBER BASED ON EMBEDDING OF DUAL RESONATORS

Pramod K. Singh[1], Shideh Kabiri Ameri[1], Liu Chao[2], Mohammed N. Afsar[2], and Sameer Sonkusale[1, *]

[1]NanoLab, Department of Electrical and Computer Engineering, Tufts University, Medford, MA 02155, USA

[2]High-Frequency Materials Measurement and Information Center, Department of Electrical and Computer Engineering, Tufts University, Medford, MA 02155, USA

Abstract—Metamaterial based electromagnetic wave absorbers provide perfect absorption only over a narrow bandwidth. In this paper, broadband response is achieved through embedding of one resonator inside another in each unit cell of the metamaterial absorber lattice. These two resonators are oriented in the same direction to achieve reduced coupling between them realizing two absorption frequencies close to each other in order to broaden the effective bandwidth. The paper presents such an absorber at 77 GHz with a bandwidth of 8 GHz and peak absorption of greater than 98%. The absorber is fabricated on 125 μm thin and flexible polyimide substrate by patterning gold thin film in the shape of two split ring resonators as the metamaterial unit cell. The bandwidth is enhanced by more than a factor of two compared to what could be achieved from a metamaterial with single resonator structure.

1. INTRODUCTION

Metamaterials are made by the inclusion of sub-wavelength metallic structures in host dielectric medium, engineered to achieve unusual properties not found in the nature. Recently, metamaterials has enabled design of thin electromagnetic wave absorbers [1]. Absorbers have many applications in radars, imaging [2], wireless communication [3], thermal imagers [4], and possibly in the solar

Received 2 July 2013, Accepted 11 September 2013, Scheduled 27 September 2013

* Corresponding author: Sameer Sonkusale (sameer@ece.tufts.edu).

cells [5]. Compared to the conventional millimeterwave absorbers which are physically thick and where frequency performance is dictated by the inherent complex permittivity [6] and permeability [7, 8] of the bulk material, metamaterial based absorbers can be tailored for frequency response through the geometry of metallic inclusions. Metamaterial absorbers are frequency selective and have already been investigated over a wide range of frequencies spanning the microwave [1], terahertz (THz) [9, 10], infrared (IR) [11], and optical [12] spectrum. Design of absorbers at millimeterwave or higher frequencies using metamaterial based approaches is frequency scalable compared to conventional bulk material based absorbers. However, bandwidth of metamaterial based absorber relies on resonance bandwidth of the resonator structure which is typically narrowband. However, one requires broad bandwidth for many of these applications. Several approaches have been investigated to design absorbers beyond single resonance. One example is that of dual band absorber demonstrated at millimeterwave frequencies [13, 14] and at THz [9, 10] frequencies. In another application, a broadband absorber at 2.4 GHz has been investigated using stacked multi frequency resonators that achieved absorption bandwidth of 700 MHz [15]. An ultra broadband absorber over a frequency range of 6–18 GHz with an absorption level of 90% has been demonstrated using frequency selective resistive surface which relies on the tuning of material resistivity [16]. Absorber at 30 GHz has also been investigated for the wideband absorption using multiple resonators [17] with purely numerical simulations; moreover the response is not flat over wideband. Another broadband absorber (7.8–14.7 GHz) is realized by using multilayered structure in the form of a pyramid which needs complex fabrication approach [18]. Broadband absorber at IR wavelength designed using multiplexed metal patches has been shown to achieve 98% absorption over 3.4–3.55 μm [19]. Broadband IR absorber is also realized using plasmonic nanoantennas with multiple resonance [20] and dual resonance [21] absorption responses.

In this paper, a metamaterial absorber at millimeterwave frequency is investigated for the absorption bandwidth enhancement at the resonant frequency. To design this absorber, a dual band absorber forms the basis wherein a second resonator with a resonance frequency close to the first resonator is embedded inside the first resonator. One observes that placing two different resonators, each with perfect absorption at their resonant frequencies, close to each other causes mutual coupling (and resonance splitting) which just degrades the overall absorption and does not yield a broadband response. In this paper we showcase a simple approach to minimize coupling between

the two resonators with resonances close to one another in frequency. Moreover each resonator by itself does not yield perfect absorption at their resonance frequencies, however the combined effect shows not just widening of the bandwidth, but also higher peak absorption than a single resonator case. Millimeterwave frequency band of 77 GHz is selected for these absorbers for their significance in automotive radar applications. Samples are fabricated on polyimide which is flexible and suitable for the conformable applications.

2. METAMATERIAL ABSORBER DESIGN

Metamaterial absorber is presented schematically in Fig. 1(a). Top layer of the absorber consists 2D periodic array of split ring resonators (SRRs) made of metals such as gold patterned on a polyimide dielectric spacer layer. The back side of the absorber is coated with a continuous thin metal layer. The simultaneous interactions of electric (in the gap of SRR) and magnetic (between SRR and backside metal) fields of incident wave with the metamaterial result in the wave impedance ($\eta = E/H = \sqrt{(\mu/\varepsilon)}$) matching of absorber to the free space at the

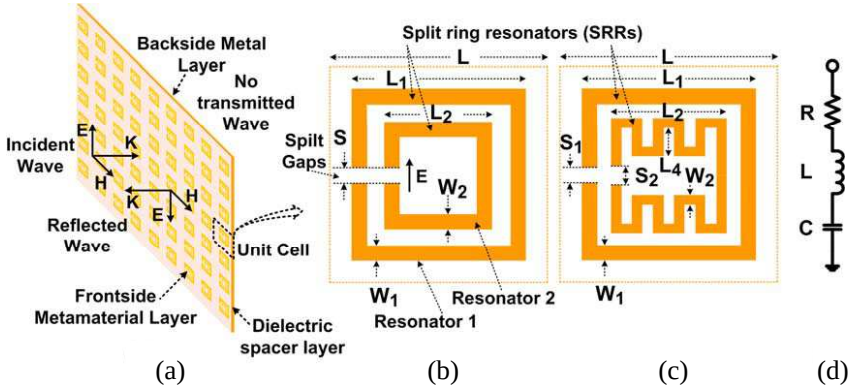

Figure 1. (a) Schematic representation of metamaterial absorber. The incident wave is reflected back and there is no transmitted wave due to backside continuous metal layer. The wave is absorbed at resonance frequency when electric field is parallel to the gap of the resonator as shown in the figure. (b) Layout of the unit cells for dual band absorber using two resonators, and (c) inner resonator is folded to increase length of the resonator for decreasing second resonance frequency and bringing that close to the first resonance frequency. (d) Circuit based (RLC) model of the single SRR resonator.

resonance frequency eliminating reflection [1]. This incident wave gets absorbed as metallic and dielectric losses at the resonance frequency. Waves in frequency other than resonance are reflected back primarily due to the presence of the backside continuous metal layer; this also implies zero transmission through the absorber.

Split ring resonator ('C' shaped) is used as the metamaterial unit cell shown in Figs. 1(b) and 1(c) with resonance frequency of 77 GHz. Another split ring resonator is inserted inside the first resonator to achieve second resonant absorption frequency. The absorption frequency of the resonator can be modeled using equivalent inductance (L) and capacitance (C) of the resonator as shown in Fig. 1(d). The resonant absorption frequency of the resonator, $f = 1/(2\pi\sqrt{(LC)})$ can be varied by changing its dimensions. The increase or decrease in the inductance value of the resonator is related to the increase or decrease in the length of the resonator, respectively. Similarly the value of capacitance can be increased or decreased by increasing or decreasing the split gap capacitance of the SRR. Since the second resonator is placed inside the first resonator, without changing its design, it will have smaller length and will therefore exhibit resonance at much higher frequency than the first resonator. In order to enhance the absorption bandwidth at a single resonant frequency the goal would be to bring the second resonance close to the first resonance so that the combination achieves broad absorption. To achieve this goal, we varied different parameters for the second resonator. Increasing effective length of the resonator through meandering was found to be more effective than trying to increase the capacitance by bringing the edges of the SRR closer or extending inside.

Absorber designs are simulated in CST Microwave Studio (2011) software. Polyimide with thickness of 125 µm ($\varepsilon = 3.16$, tand = 0.01) is used as a dielectric spacer layer. In this design no transmitted wave is observed either in simulation or in measurement due to presence of the continuous backside conductive layer. S-parameter obtained from the simulation is used to determine the power reflection coefficient ($R = S_{11}^2$). Since the transmission coefficient is zero ($T = S_{21}^2 = 0$), the power absorption coefficient (A) is directly determined from the power reflection coefficient ($A = 1 - R - T = 1 - R$).

It is important to mention that when two resonators are brought closer in space, they mutually couple to one another, altering their resonant response in a behavior commonly known as hybridization or resonant splitting [22, 23]. The extent of mutual coupling depends not only on the spacing, but also on the relative orientation (or polarity) of one resonator with respect to the other. In Figs. 2(a) and 2(b) two different resonators are used individually to achieve

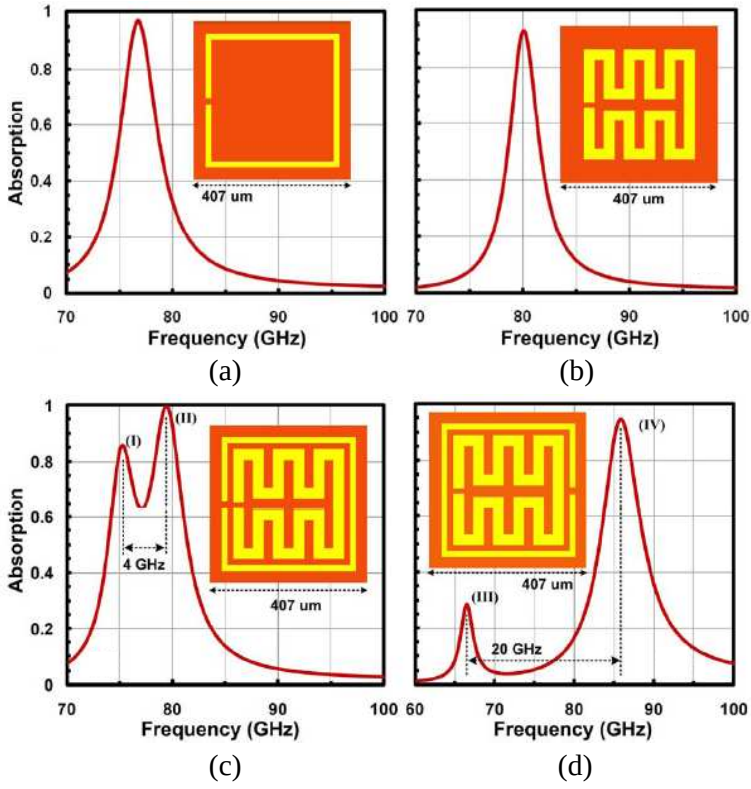

Figure 2. Dual band absorber with two absorption frequencies close to each other designed for the bandwidth enhancement. (a) Single band absorbers designed at 77 GHz and (b) at 80 GHz. (c) Embedding these two split ring resonators with the same orientation and (d) embedding in opposite orientation. Greater coupling between resonators in the case of design (d) results in larger separation of resonance frequencies compared to the design in (c) showing larger hybridization effects when resonators are embedded in the opposite directions.

absorption at frequencies 77 GHz and 80 GHz, respectively. These two resonators can be embedded in two ways, first shown in Fig. 2(c) where the split gap of both resonators is oriented on the same side; and second shown in Fig. 2(d) where resonators gap is oriented on opposite sides. The coupling between structures is much stronger when they are on opposite sides resulting in resonance splitting due to strong hybridization effects. The coupling can be observed from the induced surface currents in the resonators as shown in Figs. 3 and 4 for two

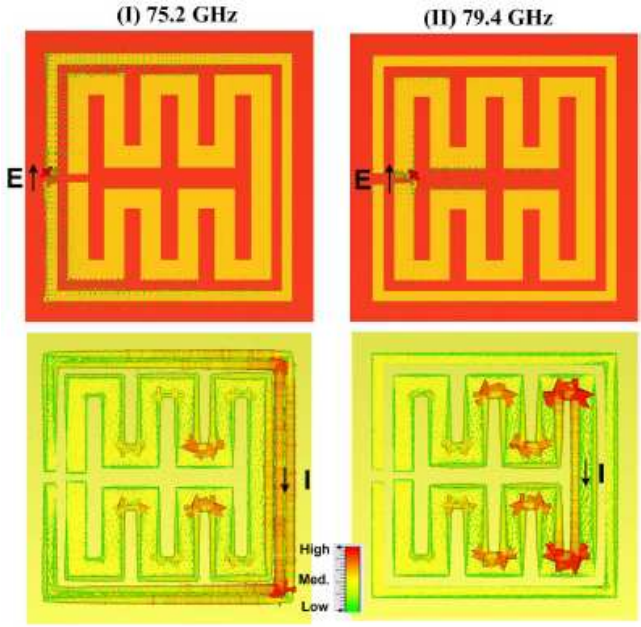

Figure 3. Induced electric field and surface current at resonance frequencies shown in Fig. 2(c). Coupling between resonators is small when both are oriented in the same direction.

different orientations of the resonators. The higher surface current is induced in both resonator at each of two resonance frequencies when they are oriented in the opposite direction as shown in Fig. 4. This coupling is highly reduced when the resonators are oriented in the same direction as shown in Fig. 3. This reduced the hybridization effects greatly and the two resonances occur very close to each other.

Further optimization of the design through numerical simulation can be performed to achieve perfect absorption over this frequency band. To demonstrate absorber with broadened bandwidth, using the proposed approach of having resonators oriented in the same direction, we present simulation results on two designs that showcase how broadening of the bandwidth is achieved. In design 1, resonance frequency corresponding to the outer resonator is selected 77 GHz and to the inner resonator 80 GHz as shown in Fig. 5(a). However, in design 2, the inner resonator frequency is selected to be much closer the first resonator (< 80 GHz) so that the combined response appears similar to the single resonator but with enhanced absorption bandwidth as shown in Fig. 5(b). In design 2, the number of folds

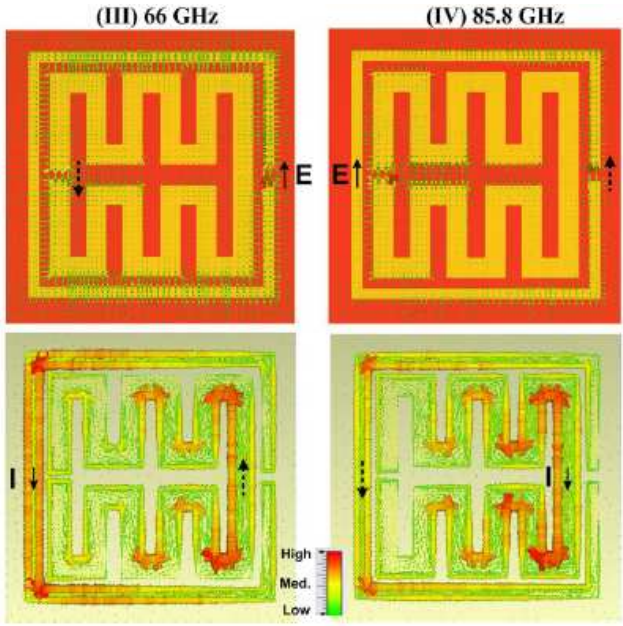

Figure 4. Induced electric field and surface current at resonance frequencies shown in Fig. 2(d). Stronger coupling between resonators is observed in comparision to the case shown in Fig. 3, even resonance frequencies are farther.

in the inner resonator is three compared to the two in design 1 to scale down second resonance frequency. These designs are optimized to achieve perfect absorption peaks at 77 GHz and 80 GHz in the case of the design 1, and peak absorption at 77 GHz with maximum bandwidth in case of the design 2. It can be observed from Fig. 5(a) that combination of two resonators results in the perfect absorption at 77.45 GHz (absorption, 99.9%) and at 80.35 GHz (absorption, 99.0%), though the absorption level of the resonators, individually is not perfect. Simulated bandwidth for an absorption level of 90% is 4.2 GHz for the design 1 and 2.7 GHz for the design 2 in comparison to the 1 GHz for the absorber designed using single resonator as shown in Fig. 5(b), indicating that large enhancement of bandwidth is possible using dual resonator structure. Fig. 6 illustrates that at 77 GHz induced electric field and surface currents due to magnetic field appears in the outer resonator and at 80 GHz it appears in the inner resonator. The absorbed power loss density on the absorber surface is shown in Fig. 7 for different frequencies.

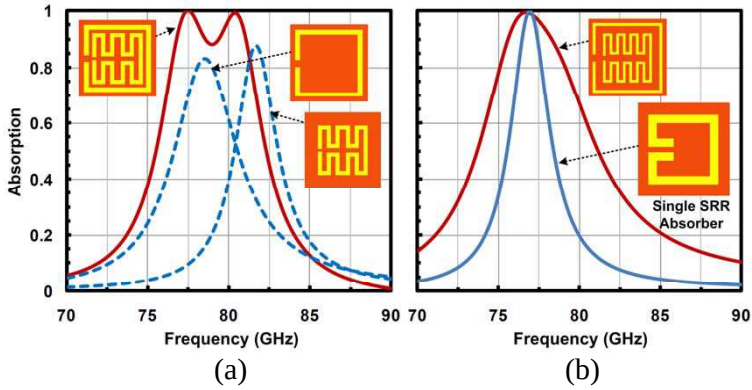

Figure 5. Two designs of absorber using dual SRRs for the enhanced bandwidth. (a) Design 1, two very close resonance absorption frequencies (77 and 80 GHz) achieved using two additional folds in the inner resonator. (b) Design 2, both resonator frequencies are close enough to appear as a single resonance absorber with enhanced bandwidth, inner resonator has three additional folds in this design. Simulated result of a separate absorber designed using single resonator is also shown for comparison of the bandwidth.

3. FABRICATION AND MEASUREMENTS

Absorber samples shown in Fig. 5 (design 1 and 2) are fabricated using standard optical photolithography process. Silicon wafers with 4 inch diameter are used as the supportive substrate. Polyimide film as dielectric spacer layer of the metamaterial absorber is prepared on silicon wafer. Metamaterial patterns are transferred on the Polyimide using the lithography process. Chromium and gold metals serving as metamaterial layer are deposited using a DC sputtering system with thickness of 20 nm and 200 nm, respectively. Polyimide film is peeled off from the silicon wafer after fabrication of metamaterial layer. Chromium and gold layers are then coated on the back side of sample to form a continuous conducting back plane.

Measurement of the samples is performed using custom made spectrometer, shown in Fig. 8. Backward wave oscillator (BWO) is used as a millimeterwave source in the spectrometer. The frequency of the BWO is voltage tuned in the range of 70–117 GHz. To detect signal power, a Schottky diode detector is used. Incident wave is modulated to facilitate lock-in based detection. The spectrometer is a free space measurement setup utilizing lenses and beam splitter. Samples are measured in reflection mode at normal incidence. To normalize

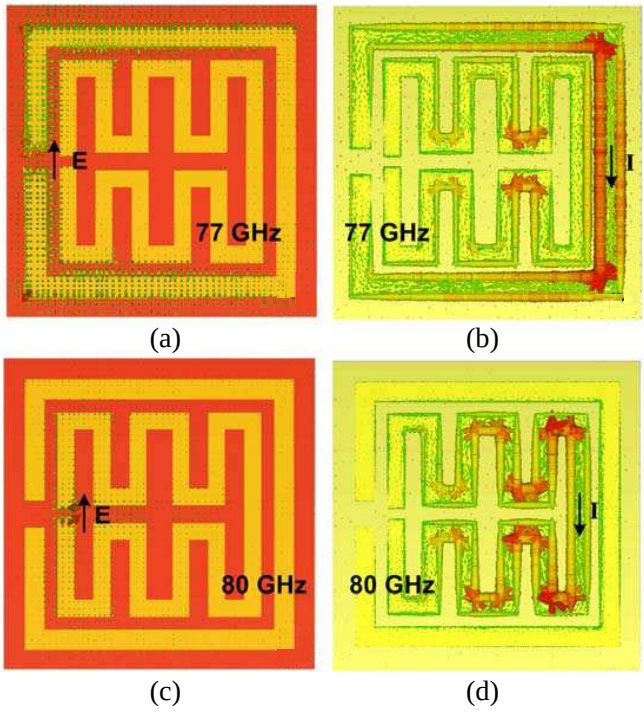

Figure 6. Simulated electric field, surface current of absorber in design 1. (a) Electric field induced in the gap of outer resonator at 77 GHz due to coupling of electric field component of the incident wave. (b) Surface current is induced in the resonator by magnetic field component of the wave between resonator and ground plane. (c), (d) Electric field and surface current induced in the inner resonator at 80 GHz.

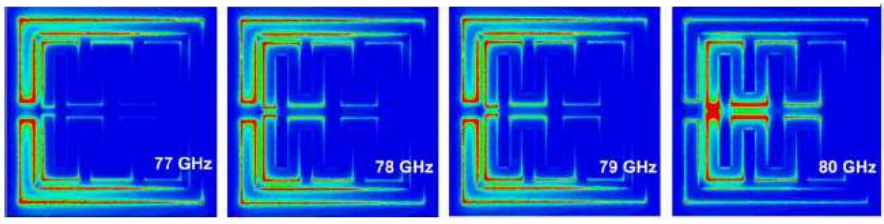

Figure 7. Simulated power loss density at different frequencies in the absorption band of the absorber in design 1.

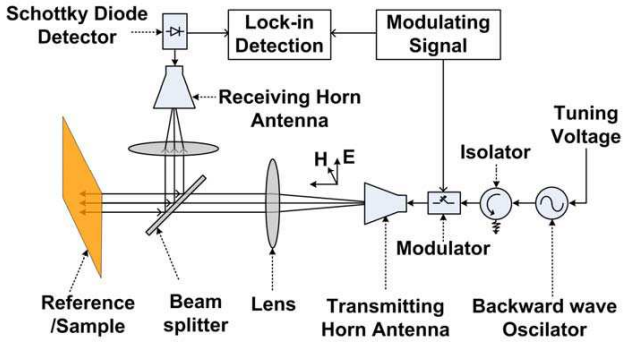

Figure 8. Setup for the measurement of reflection coefficient of the absorber.

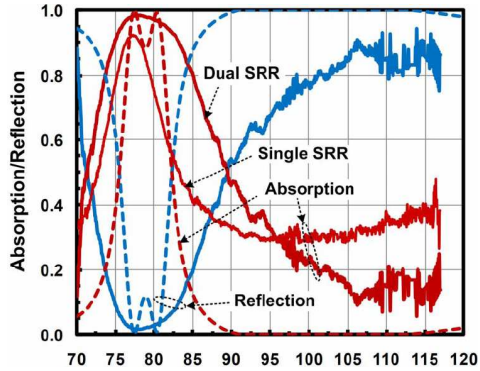

Figure 9. Simulated (dotted lines) and measured (continuous lines) power absorption and reflection coefficients of bandwidth enhanced metamaterial absorber using dual SRR (design 1). Result of metamaterial absorber designed using single SRR at 77 GHz is given for the comparison. Dimensions are; $L_1 = 352\,\mu m$, $L_2 = 266\,\mu m$, $L = 407\,\mu m$, $W_1 = 26\,\mu m$, $W_2 = 22\,\mu m$, $S_1 = 36\,\mu m$, $S_2 = 15\,\mu m$, and $L_4 = 99\,\mu m$ for the structure shown in Fig. 1.

observed measurement, a reference measurement is performed using a perfect metal plate reflector. The measured response of the absorber is shown in Fig. 9 for the design 1. The maximum measured absorption in this absorber is 98% over a frequency range of 77.15–78.80 GHz. Absorption bandwidth for absorption value greater than 90% is 74.95–83.20 GHz (8.25 GHz or 10%). Measured response of the metamaterial absorber using single resonator is also shown in Fig. 9 for

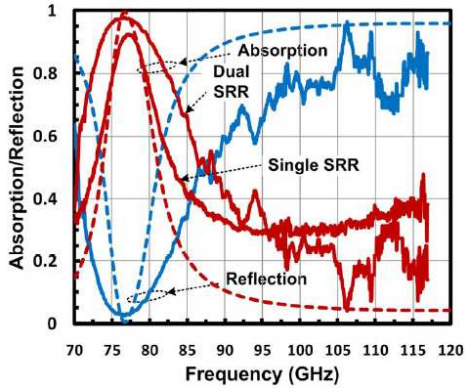

Figure 10. Simulated (dotted lines) and measured (continuous lines) power absorption and reflection coefficients of bandwidth enhanced metamaterial absorber using dual SRR (design 2). Absorber using single SRR at 77 GHz is given for the comparison. Dimensions are $L_1 = 342\,\mu m$, $L_2 = 240\,\mu m$, $L = 386\,\mu m$, $W_1 = 14.8\,\mu m$, $W_2 = 13\,\mu m$, $S_1 = 34\,\mu m$, $S_2 = 23.4\,\mu m$ and $L_4 = 90\,\mu m$ for the structure shown in Fig. 1.

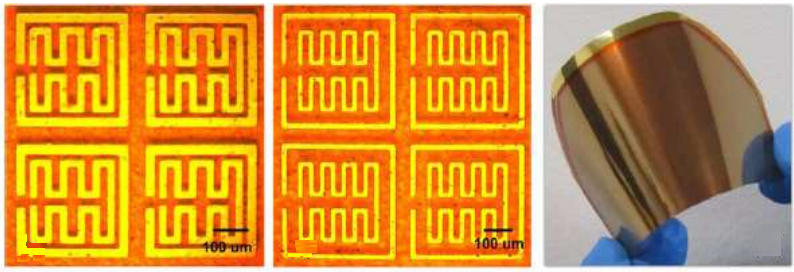

Figure 11. Microscopic images of the fabricated metamaterial absorber samples. (a) Design 1. (b) Design 2. (c) Photo of the absorber sample showing its flexibility.

the comparison and showing that absorption bandwidth of absorber designed using dual resonator is much higher (greater than 2 times for the absorption value of 80%) than the absorber designed using single resonator. The measured response of the absorber in design 2 is given in Fig. 10. Measured maximum absorption is 97% at frequency 77.10 GHz. The absorption level of 90% or greater is achieved over a frequency range of 73.65–79.95 GHz (bandwidth of 6.3 GHz or 8%).

The absorption frequency resulted from the measurement is in good agreement with simulation. However, measured absorption bandwidth is much higher than what is observed in simulation. This is expected due to fabrication variations in unit cell dimensions across the sample, which provides a beneficial effect of broadening the overall response. Microscopic images of the two absorber samples (design 1 & 2) are shown in Figs. 11(a) and (b). Samples are flexible as shown in Fig. 11(c) and can be used for the conformable applications.

4. CONCLUSIONS

In conclusion, metamaterial based absorbers with broad bandwidth at millimeter wave frequencies are designed using two resonators, one embedded inside another. Measurement results on fabricated samples show an increase of absorption bandwidth by a factor of two compared to the single resonator case. Designs show a novel approach to orient the resonators in the same direction such that mutual coupling is minimized and no significant hybridization effects are seen. Implemented absorbers are ultra thin (1/30th of the wavelength) and flexible. These metamaterial based absorbers can be scaled to other frequencies from RF to THz covering various applications in WiFi, automotive radars, radomes, and point-to-point wireless communications.

ACKNOWLEDGMENT

Authors acknowledge funding from Office of Naval Research (ONR) through grant N00014-09-1-1075. Devices were fabricated at Tufts Micro- and Nano-fabrication facility (TMNF).

REFERENCES

1. Landy, N. I., S. Sajuyigbe, J. J. Mock, D. R. Smith, and W. J. Padilla, "Perfect metamaterial absorber," *Phys. Rev. Lett.*, Vol. 100, 207402-1–207402-4, 2008.
2. Noor, A. and Z. Hu, "Metamaterial dual polarised resistive hilbert curve array radar absorber," *IET Microw. Antennas Propag.*, Vol. 4, 667–673, 2010.
3. Takimoto, Y., "Considerations on millimeter-wave indoor LAN," *Topical Symposium on Millimeter Waves*, 111–114, 1997.

4. Maier, T. and H. Bruckl, "Wavelength-tunable microbolometers with metamaterial absorbers," *Optics Letters*, Vol. 34, 3012–3014, 2009.
5. Aydin, K., V. E. Ferry, R. M. Briggs, and H. A. Atwater, "Broadband polarization-independent resonant light absorption using ultrathin plasmonic super absorbers," *Nature Communications*, Vol. 2, Article No. 517, DOI: 10.1038/ncomms1528.
6. Takase, Y., O. Hashimoto, K. Matsumoto, and T. Kumada, "Suppression of electromagnetic radiation noise from wireless modules in the millimeter-wave band by means of alumina containing carbon black," *Electronics and Communications in Japan*, Vol. 93, 25–33, 2010.
7. Iijima, Y., Y. Hoqjou, and R. Sato, "Millimeter wave absorber using M-type hexagonal ferrite," *IEEE International Symposium on Electromagnetic Compatibility*, Vol. 2, 547–549, 2000.
8. Korolev, K. A., J. S. McCloy, and M. N. Afsar, "Ferromagnetic resonance of micro- and nano-sized hexagonal ferrite powders at millimeter waves," *J. Appl. Phys.*, Vol. 111, 07E113-1–07E113-3, 2012.
9. Wen, Q.-Y., H.-W. Zhang, Y.-S. Xie, Q.-H. Yang, and Y.-L. Liu, "Dual band terahertz metamaterial absorber: Design, fabrication, and characterization," *Appl. Phys. Lett.*, Vol. 95, 241111-1–241111-3, 2009.
10. Tao, H., C. M. Bingham, D. Pilon, K. Fan, A. C. Strikwerda, D. Shrekenhamer, W. J. Padilla, X. Zhang, and R. D. Averitt, "A dual band terahertz metamaterial absorber," *J. Phys. D: Appl. Phys.*, Vol. 43, 225102-1–225102-5, 2010.
11. Mason, J. A., S. Smith, and D. Wasserman, "Strong absorption and selective thermal emission from a midinfrared metamaterial," *Appl. Phys. Lett.*, Vol. 98, 241105-1–241105-3, 2011.
12. Hao, J., J. Wang, X. Liu, W. J. Padilla, L. Zhou, and M. Qiu, "High performance optical absorber based on a plasmonic metamaterial," *Appl. Phys. Lett.*, Vol. 96, 251104-1–251104-3, 2010.
13. Soh, T., A. Kondo, M. Toyota, and O. Hashimoto, "A basic study of millimeter-wave absorber for two frequency bands using transparent resistive films," *IEEE International Symposium on Electromagnetic Compatibility*, Vol. 1, 149–154, 2003.
14. Singh, P. K., K. A. Korolev, M. N. Afsar, and S. Sonkusale, "Single and dual band 77/95/110 GHz metamaterial absorbers on flexible polyimide substrate," *Appl. Phys. Lett.*, Vol. 99, 264101-1–264101-4, 2011.

15. Gu, S., J. P. Barrett, T. H. Hand, B.-I. Popa, and S. A. Cummer, "A broadband low-reflection metamaterial absorber," *J. Appl. Phys.*, Vol. 108, 064913-2–064913-6, 2010.
16. Sun, L. K., H. F. Cheng, Y. J. Zhou, and J. Wang, "Broadband metamaterial absorber based on coupling resistive frequency selective surface," *Optics Express*, Vol. 20, 4675–4678, 2012.
17. Wakatsuchi, H., S. Greedy, C. Christopoulos, and J. Paul, "Customised broadband metamaterial absorbers for arbitrary polarisation," *Optics Express*, Vol. 18, 22187–22198, 2010.
18. Ding, F., Y. Cui, X. Ge, Y. Jin, and S. He, "Ultra-broadband microwave metamaterial absorber," *Appl. Phys. Lett.*, Vol. 100, 1035061-1–1035061-4, 2012.
19. Hendrickson, J., J. Guo, B. Zhang, W. Buchwald, and R. Soref, "Wideband perfect light absorber at midwave infrared using multiplexed metal structures," *Optics Letters*, Vol. 37, 371–373, 2012.
20. Bouchon, P., C. Koechlin, F. Pardo, R. Haidar, and J.-L. Pelouard, "Wideband omnidirectional infrared absorber with a patchwork of plasmonic nanoantennas," *Optics Letters*, Vol. 37, 1038–1040, 2012.
21. Koechlin, C., P. Bouchon, F. Pardo, J.-L. Pelouard, and R. Haıdar, "Analytical description of subwavelength plasmonic MIM resonators and of their combination," *Optics Express*, Vol. 21, 7025–7032, 2013.
22. Guo, H., N. Liu, L. Fu, T. P. Meyrath, T. Zentgraf, H. Schweizer, and H. Giessen, "Resonance hybridization in double split-ring resonator metamaterials," *Optics Express*, Vol. 19, 12095–12101, 2007.
23. Aydin, K., I. M. Pryce, and H. A. Atwater, "Symmetry breaking and strong coupling in planar optical metamaterials," *Optics Express*, Vol. 18, 13407–13417, 2010.